Available online at www.sciencedirect.com
SCIENCE DIRECT®
Thermochimica Acta 434 (2005) 74–80
thermochimica acta
www.elsevier.com/locate/tca

Reducibility, heats of re-oxidation, and structure of vanadia supported on TiO_2 and TiO_2–Al_2O_3 supports used as vanadium traps in FCC

Silvia Martínez [a], Rosario Morales [a], Maria Guadalupe Cárdenas-Galindo [a], A. Gabriel Rodríguez [b], Francisco Pedraza [c], Brent E. Handy [a,*]

[a] *CIEP/Facultad de Ciencias Químicas, Universidad Autónoma de San Luis Potosí, Av. Dr. Manuel Nava #6, Zona Universitaria, CP 78210 San Luis Potosí, SLP Mexico, Mexico*
[b] *Instituto de Investigaciones en Comunicaciones y Opticas, Universidad Autónoma de San Luis Potosí, Av. Karakorum #1470, CP 78216 San Luis Potosí, SLP Mexico, Mexico*
[c] *Instituto Mexicano del Petróleo, Eje Centrale Lázaro Cárdenas #152, Col. San Bartolo Atepehuacán, Delg. Gustavo I. Madero, México DF 07730, Mexico*

Received 8 July 2004; received in revised form 20 January 2005; accepted 26 January 2005
Available online 24 February 2005

Abstract

V/TiO_2 and V/TiO_2–Al_2O_3 (1:1 w/w basis) supports were characterized by TPR, Raman spectroscopy, and heats of re-oxidation of samples pre-reduced in CO at 770 K with a heat-flow calorimeter. Supports were pure anatase or rutile dispersed with hydrated aluminas (boehmite, gibbsite, bayerite) subsequently calcined at 870 K. Raman spectroscopy of fully oxidized, air-exposed samples show the presence of polymeric polyvanadate species, but not of isolated monomeric species. Sample loadings were 4 wt.% and show different reduction and structural features. During TPR, vanadia reduced to V(III) and V(IV) in V/rutile and V/anatase, respectively, and multiple reduction peaks were observed due to crystalline V_2O_5 and amorphous vanadia. In V/TiO_2–Al_2O_3 samples, vanadium coverages were 6–8 μmol V m^{-2} yielding well-dispersed, amorphous vanadia. Trends observed during TPR were: addition of bayerite phase to anatase or rutile increases H_2 consumption by 100%, implying formation of V(III) and V(II), respectively. However, with addition of boehmite or gibbsite to either titania phase, vanadia reduces only to V(IV). Oxygen doses at 473 K of pre-reduced samples titrated about one-third of total vanadia content. Re-oxidation heat values range from 400 to 500 kJ mol^{-1} O_2 and represent oxygen–vanadium ion bond strengths within the dispersed vanadia. The heat values are higher than expected for re-oxidation of a bulk phase, and are indicative of the degree of stabilization provided by the support.

Keywords: Calorimetry; TPR; Vanadia; Titania; Alumina; Titania–alumina

1. Introduction

Vanadium is a common metal contaminant of heavy distillation residues that poisons the catalytically important zeolite component of the FCC catalyst by entering its micropores and accelerating the dealumination and destruction of the faujasite structure. The poisoning mechanism involves the reaction of vanadium oxidic species with high temperature steam during the regeneration stage during FCC, forming vanadic acid that attacks the aluminum and silicon sites within the faujasite framework [1]. Traditionally, transition metal levels in the equlibrium FCC catalyst have been kept tolerable by removing resids from the gasoil feedstock, yet in the interest of increasing gasoline yields per barrel of crude, and as low sulfur crude stocks are becoming depleted, it has become necessary to include increasing amounts of resid in the FCC feed. This issue is of particular importance to Mexico, which will

* Corresponding author. Tel.: +52 444 826 2440; fax: +52 444 826 2372.
E-mail address: handy@uaslp.mx (B.E. Handy).

0040-6031/$ – see front matter © 2005 Elsevier B.V. All rights reserved.
doi:10.1016/j.tca.2005.01.055

rely principally on the Maya crude oil deposits for its energy needs in the coming decades. The Maya crude feedstock [2] unfortunately contains among the highest contents of sulfur and metals content of any feedstock available. The principal strategy of preventing vanadium poisoning of the FCC catalyst, as noted in the recent patent literature [3], is to retard or prevent vanadium species from entering the zeolite pores by adding a refractory ingredient, typically a spinel phase or basic oxide, that can bind strongly with the vanadium, yet not be catalytically active to adversely affect the product composition. The immobilization of vanadium may be due to the formation of stoichiometric or non-stoichiometric mixed metal oxide phases or solid solutions, whose exact composition may depend on a number of factors, such as metal concentrations, support synthesis, thermal pre-treatments, the presence of stabilizing anions. The objective of this work was to probe the redox properties of vanadia supported on several V-traps prepared from titania and titania–alumina, and hopefully gain more insight into the V-support interaction operative on these materials.

2. Experimental

2.1. Sample preparation

The titania supports used were either pure anatase (A) phase (Sachtleben Chemie, 100 $m^2\ g^{-1}$) or a pure rutile (R) phase, prepared by a precipitation method reported previously [4]. Mixed titania–alumina supports were prepared by mechanically dispersing equal amounts (weight basis) of pure titania (A or R) with one of three commercial, hydrated aluminas (Engelland Intercat) of the phases boehmite, gibbsite, and bayerite, identified here as C, G, and B, respectively. Prior to mixing with the titania component, a portion (20%) of the alumina component was peptized to impart mechanical resistance to the resulting particles. The peptization procedure employed was similar to that described by Magee and Mitchell [5], dispersing the 20% alumina portion in 1 N HNO_3. The remaining 80% portion was mechanically mixed with the titania component and then gradually added to the peptidized solution, after which the temperature was raised to 343 K and held under constant agitation until the water evaporated completely. The sample was further dried at 373 K for 4 h and calcined by heating at 4 K min^{-1} to 870 K over an additional 4-h period. Powder X-ray diffraction analysis of all calcined samples show that in all samples the alumina component formed γ-alumina crystallites, and that the crystal structure of the starting titania component was retained. The BET surface areas of the mixed oxides ranged from 92 to 116 $m^2\ g^{-1}$. Vanadium-impregnated samples of ca. 3 wt.% loading were prepared by the incipient wetness method, using a solution of ammonium metavanadate–oxalic acid (1:2 ratio). The samples were dried for 5 h at 423 K and then calcined at 770–813 K for 4 h. Vanadium content and surface area data are summarized in Table 1.

2.2. Characterization

Temperature-programmed reduction experiments were conducted using a 4 mm i.d. quartz reactor tube, with exit stream connected to a Chrompak MicroGC capable of analyzing gas concentrations within intervals of 30 s. Sample size was 0.1 g in each case, and each run was performed at a heating rate of 10 K min^{-1} in 5% H_2/Ar flowed at 100 $cm^3\ min^{-1}$. Prior to TPR, samples were pre-oxidized in pure oxygen at 100 $cm^3\ min^{-1}$ for 30 min at 870 K and cooled under oxygen flow to room temperature, after which the gas was switched to the reducing gas. Heats of re-oxidation of pre-reduced samples were obtained using a homemade Tian–Calvet calorimeter system similar to that described elsewhere [6]. In brief, this instrument consisted of four components: (i) a calorimeter unit, consisting of two custom-designed heat-flux transducers (ITI Co., Del Mar, CA, USA) within a stainless steel heat sink capable of being heated and maintained to 473 K; (ii) stainless steel dosing section equipped with two capacitance manometers (MKS Instruments, Billerica, MA, USA) for measuring dosing and equilibration pressures; (iii) oil diffusion pump system backed by mechanic pump and capable of maintaining the system at 10^{-4} Pa under dynamic pumping; (iv) high purity dosing and treatment gas storage system consisting of 5-l spheres with glass high vacuum stopcocks. Helium, hydrogen, and carbon monoxide were purified by flowing through copper turnings trap heated to 548 K followed by activated 5 A MS trap maintained at 196 K. Quartz sample cells (20 mm o.d., 20 mm height) were loaded with ca. 0.5 g finely ground sample powder. The sample was pre-reduced by heating under vacuum (10^{-3} Pa) to 770 K and then exposing the sample to several 0.67 kPa doses of hydrogen or carbon monoxide, evacuating the cell after 5 min of exposure to each dose, and then exposing the sample to one 33 kPa dose for 30 min, after which the sample was evacuated, allowed to cool, and inserted in the calorimeter unit to stabilize at 473 K. Heats of re-oxidation were performed at 473 K with small doses (0.2–1 kPa) of oxygen, introduced in succession, until the heat response was too small to measure. Equilibration times between doses were 30–45 min. Heat-flow signals were amplified and recorded by computer using data-acquisition software (LABVIEW) and quantified by previous calibration with a powdered sample of known heat yield. Gas consumption for each dose was determined as the difference between initial and final amounts of gas present in dosing section (20 cm^3) and cell headspace (25 cm^3), the latter of which was determined at the end of each run using helium. Differential heat plots were formed by dividing the specific heat yield per dose by the amount of gas consumed in each dose. Laser Raman spectroscopy was performed using a Jobin–Yvon T6400 spectrometer equipped with a triple-pass monochromator, CCD detector, and a laser excitation wavelength of 514.5 nm. The illumination area was 10 μm, and spectra were collected with three scans over a 60 s period at a resolution of 0.5 cm^{-1}.

Table 1
Surface area and vanadium content

Sample	BET area ($m^2\,g^{-1}$)	V_2O_5 (%)	V (%)	V loading ($\mu mol^{-1}g$)	V coverage ($\mu mol\,m^{-2}$)
A	67	6.19	3.47	681	10.2
AB	116	6.90	3.87	760	6.5
AG	92	6.92	3.88	762	8.3
R	32	6.16	3.45	677	21.2
RB	110	6.43	3.60	707	6.4
RC	112	6.80	3.81	748	6.7
RG	113	6.70	3.75	736	6.5

3. Results and discussion

3.1. Temperature-programmed reduction

TPR profiles for the seven samples studied are shown in Fig. 1. Reduction of vanadia supported on the five TiO_2–Al_2O_3 samples is registered by a single broad reduction peak. The mixed oxides containing rutile (RB, RG, RC) have peak maxima centered at 793–795 K, whereas the anatase-containing mixed oxides AG and AB have reduction peaks centered at 801–803 K. The location of T_{max} are generally dependent upon support type and vanadia loading [7]. Since there is only slight variation in the latter parameter amongst these samples, it is likely that the anatase component is responsible for the higher T_{max} values. On the other hand, the V/A and V/R samples show multiple reduction peaks. The pure anatase-supported vanadia showed an early onset of reduction at 668 K, a major component peak centered at 794 K, and a high temperature reduction centered at 938 K. In the rutile-supported vanadia sample, the reduction formed a principal peak centered at 793 K, but contained a high temperature shoulder to this peak, centered at 838 K. Although the V loadings in these samples are similar to those in the TiO_2–Al_2O_3 supports, there was notable particle sintering in the pure titania supports during the thermal treatments, decreasing the surface area and hence yielding considerably higher vanadia surface densities. It has been reported [8] that there is a theoretical monolayer capacity of 0.1 wt.% $V_2O_5\,m^{-2}$ of support surface, which corresponds to about 11 $\mu mol\,V\,m^{-2}$. This capacity was indeed exceeded with V/R and V/A is near this limit, thus bulk V_2O_5 particles were formed along with a dispersed vanadia phase. This was confirmed by the Raman data, which are discussed below. Hydrogen consumption levels during TPR are shown in Table 2. Again, it should be noted that the vanadium loading is approximately the same in all samples. Yet the H_2 consumption of V/R is twice that of V/A. Comparison of consumption levels with the theoretical H_2 consumption suggests that fully oxidized vanadia reduces to V(IV) in V/A and to V(III) in V/R. In the TiO_2–Al_2O_3 supports, the combination of bayerite with either anatase or rutile leads to a two-fold increase in H_2 consumption relative to the consumption levels experienced with vanadia supported on each respective pure titania support. The implication is that V(V) reduces to V(III) in V/AB and nearly down to V(II) in V/RB. The mixing of gibbsite or boehmite with anatase or rutile components does not lead to major changes in vanadium reducibility. In these cases, the H_2 consumption levels suggest reduction of V(V) to V(IV). The multiple reduction peaks in V/A and V/R are due to the presence of different forms of vanadia, crystalline V_2O_5 being one of them. Yet multiple reduction peaks can also result from a process that is stagewise, which has been shown to be clearly the case with bulk V_2O_5. In the work of Bosch et al. [9] three prominent reduction peaks were found and attributed to the three-step reduction process.

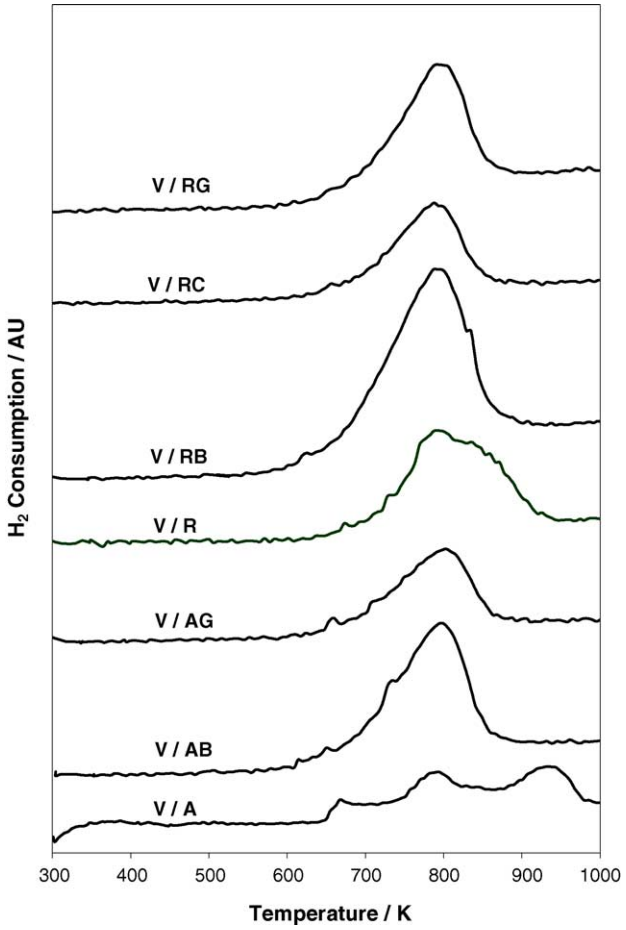

Fig. 1. TPR Profiles of V/TiO_2 and V/TiO_2–Al_2O_3 samples.

$$V_2O_5 \rightarrow 1/3\,V_6O_{13} \rightarrow 2\,VO_2 \rightarrow V_2O_3$$

Table 2
H_2 consumption and vanadium content in TPR experiments

Sample	V (%)	V loading (μmol g^{-1})	H_2 concentratios (μmol g^{-1})	Theoretical H_2 concentrations (μmol g^{-1})		
				$V^V \rightarrow V^{IV}$	$V^V \rightarrow V^{III}$	$V^V \rightarrow V^{II}$
A	3.47	681	563	681	1362	2044
AB	3.87	760	1180	760	1519	2279
AG	3.88	762	784	762	1523	2285
R	3.45	677	1205	677	1354	2032
RB	3.60	707	2030	707	1413	2120
RC	3.81	748	638	748	1496	2244
RG	3.75	736	886	736	1472	2208

whereupon V(V) → V(V,IV) → V(IV) → V(III). The 793 K peak appearing in both V/A and V/R is the same as these peaks appearing in the other samples, and likely corresponds to a dispersed vanadia species. Given that crystalline V_2O_5 reduces at higher temperatures, it is likely that these crystals are responsible for the 838 K shoulder peak in V/R and the 938 K peak in V/A. The lower temperature of the shoulder peak in V/R implies a greater degree of interaction between the V_2O_5 crystallites and the rutile particles than in V/A.

3.2. Raman spectroscopy

Raman spectra for the samples (fully oxidized state) are shown in Fig. 2. Most prominent are the strong and broad phonons for anatase (640, 519, and 398 cm^{-1}) and rutile (609, 441, and 240 cm^{-1}), where each phase is present [10,11]. Crystalline V_2O_5 is identifiable from anatase and rutile by phonons appearing at 996, 706, 533, 308, and 285 cm^{-1} [12], and these are evident in the spectra of V/A and V/R. All samples were air-exposed during the analysis, thus the surface vanadia species are likely to be hydrated or even covered by a monolayer of moisture. Notably missing from these spectra is the presence of an intense peak at 1015–1030 cm^{-1} attributable to the vanadyl stretch band of isolated, monomeric vanadia species. Instead, there is a very broad, weak maximum centered at 995 cm^{-1}, and in rutile-containing supports a similarly weak band at about 830 cm^{-1}. Both features may be due to, respectively, vanadyl stretch and V–O–V vibrations in dispersed polymeric vanadia species. Bands attributed to dispersed vanadia will shift and appear more intensely when dehydrated, although this experiment was not possible to perform with the equipment available.

3.3. Re-oxidation calorimetry

Heats of re-oxidation at 473 K are shown for all samples in Fig. 3, using CO as the reducing gas during the pre-reduction. In earlier experiments, the samples had been pre-reduced in hydrogen, and with several samples there was a notable amount of gas released during the oxygen dosing procedure, presumably water formed by the reaction of dosed oxygen with a residual amount of hydrogen that had been trapped during reduction and not degassed from the sample. This was evidenced by increases in heat yields as dosing progressed, and appeared to be an activated process, assessed by the unusually broad heat response peaks and persistent gas emission rate with time, as monitored by the precision pressure gauges. Reduction with carbon monoxide at 770 K was considered to be adequate to reduce the vanadia species to the same average oxidation state achieved with hydrogen, yet not leave molecular or atomic residues on the sample surface that may be titrated by oxygen at 473 K or higher. The mechanism of hydrogen trapping is under investigation. The initial differential heat values ranged from 430 to 600 kJ mol^{-1} (molecular oxygen basis), decreasing to between 400 and 500 kJ mol^{-1} O_2. Higher heat values on average (470 kJ mol^{-1}) were recorded for V/RB, V/RG, and V/AB and lower average values were observed for V/RC and to a certain extent V/A (400 kJ mol^{-1}). The highest heat values (500–600 kJ mol^{-1}) recorded correspond to the first two doses for V/R, in which amongst all samples the large H_2 consumption amount during the TPR experiment suggest that vanadia may have reached the oxidation state V(II). In general, the differential heat values decline with increasing oxygen uptake, dropping off rapidly for total oxygen consumption levels beyond 80 μmol g^{-1}, and a final oxygen residual pressure of about 1 kPa. The final point registered for V/R was left to equilibrate for 12 h and gave a barely detectable heat peak too broad to quantify. Comparison of total oxygen uptake at 473 K with total vanadium content and hydrogen consumption amounts from TPR are tabulated in Table 3. Although there are differences between the techniques, several observations can be made. If re-oxidation of vanadia at 473 K were completely reversible, one would expect a O_2/H_2 ratio of 0.5 for any oxidation state achieved by vanadia during the pre-reduction step. Clearly, the O_2/V ratios are considerably smaller than 0.5 in all samples, showing that the oxygen is only able to titrate between 20 and 38% of the total vanadia present. The V species most likely being titrated correspond to those that reduce in TPR below 800 K. The O_2/H_2(TPR) ratios are also low and reflect several issues: with V/RB, this ratio is half the O_2/V value due to the unusually large H_2 TPR consumption level caused by a presumed H trapping capacity of this support material during H_2 treatment. V/R has a similar O_2/H_2(TPR) ratio, for either the same reason or because the crystalline V_2O_5 in this sample did not pre-reduce with the CO treatment at 770 K. Crystalline V_2O_5 is

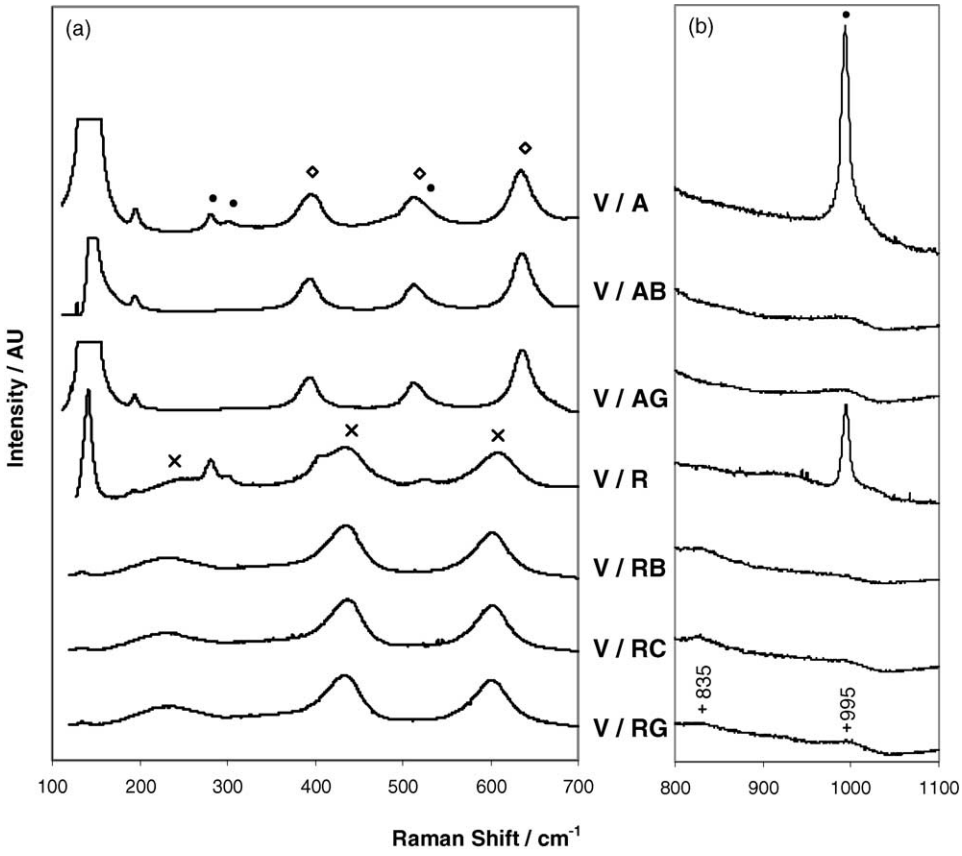

Fig. 2. Raman spectroscopy of oxidized V/TiO_2 and V/TiO_2–Al_2O_3 samples: (a) 100–700 cm^{-1} region; (b) 800–1100 cm^{-1}, amplified 3× for detail. (◊): anatase, (×): rutile, (●) crystalline V_2O_5.

also present in V/A, yet O_2/H_2(TPR) is higher than O_2/V, which may be due to a minority amount of the un-reduced V_2O_5 and the presence of more easily reducible V species, marked by the lowest temperature reduction peak of any of the samples studied. Perhaps the closest correspondence between TPR and re-oxidation calorimetry experiments exists with the samples V/AG, V/RC, and V/RG, since their TPR profiles are similar, showing maximum reduction rate near the 770 K pre-reduction temperature used in the calorimetry experiment, and vanadia reduces to V(IV) in all three. Only one-third of the reduced vanadia species re-oxidizes at 473 K (V(IV) → V(V)) in these samples. Calorimetric studies are in progress at 673 K to see if the extent of re-oxidation of vanadia is higher at this temperature.

4. Reducibility and structure of supported vanadia

A considerable number of studies have concerned the reducibility of vanadia supported on different supports. On pure titania supports, at high vanadia surface densities, crystalline V_2O_5 co-exists with a dispersed phase of polyvanadates [8]. The same type of dispersed species may be present in the TiO_2–Al_2O_3 samples, where vanadia surface densities are low enough to not form bulk V_2O_5. The dispersed phase corresponds in TPR to the reduction peaks centered at 793 K, and its structure can be identified by the weak Raman bands located above 700 cm^{-1} and below 1000 cm^{-1}. The absence of a vanadyl stretch band (V = O) in the 995–1030 cm^{-1} shift region rules out the existence of isolated monomeric vanadyl

Table 3
Oxygen consumption during re-oxidation at 473 K of samples pre-reduced at 770 K in CO

Sample	V (%)	V loading (μmol g^{-1})	O_2 consumed (μmol g^{-1})	O_2 consumed/V content	O_2 consumed /H_2 consumed (TPR)
A	3.47	681	130	0.19	0.23
AB	3.87	760	100	0.13	0.08
AG	3.88	762	135	0.18	0.17
R	3.45	677	65	0.10	0.05
RB	3.60	707	100	0.14	0.05
RC	3.81	748	115	0.15	0.18
RG	3.75	736	116	0.16	0.13

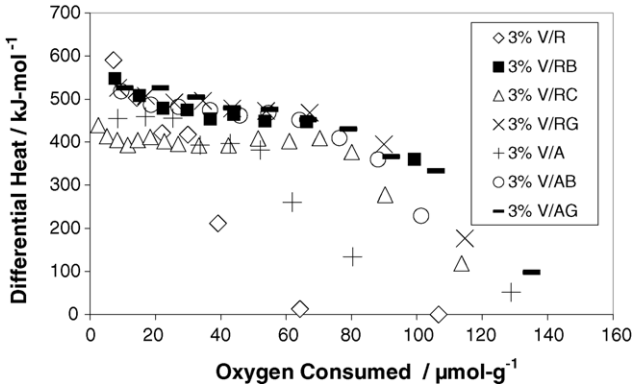

Fig. 3. Differential heats of re-oxidation at 473 K. Samples were pre-reduced at 770 K in CO gas.

species, which are typically found at low surface densities in V/SiO_2, but not normally in V/TiO_2 at any surface density level [10,11,13]. Thus, the polyvanadate structure likely consists of inter-linked VO_4 subunits with an abundance of bridge-bonded oxygens (V–O–V) but without vanadyl terminal groups. It is also possible that given the presence of room moisture during Raman studies, there is an abundance of terminal hydroxyl groups attached to V cations in the dispersed phase.

The calorimetric studies were limited to a maximum temperature of 473 K due to equipment limitations in operating temperature. It is clear from the total oxygen uptakes of all samples that this temperture was too low to re-oxidize completely the supported vanadia. As mentioned in the previous section, in the samples where vanadia was reduced to the +4 state, the O_2 uptakes represent only one-third of total V content, and in samples (i.e. V/R) where the degree of reduction was deeper, the re-oxidation amount is even less than this. Despite this, it is still possible to interprete re-oxidation heats in terms of the vanadia–oxygen bond strengths. Studies by Anderson and Kung [14] with high temperature calorimetry of V/Al_2O_3 catalysts show that re-oxidation heats correlate strongly with degree of V reduction, as well as with V loading. In their study, the supported vanadia reduced from V(V) to V(IV). From this starting point of V(IV), samples with low V coverages gave initial heats of re-oxidation of 200 kJ mol O^{-1} (400 kJ mol $O_2{}^{-1}$). With each O_2 dose, their heat values declined slightly at first, then significantly approached zero as re-oxidation became complete. In high V coverage samples, initial heats were lower (170 kJ mol O^{-1}) with each oxygen dose, although the heats recorded near complete oxidation were higher than with the low coverage samples. Such behavior could be explained by the formation of particle agglomerates of partially reduced vanadia, which are then re-dispersed upon re-oxidation, a feature that may be operative on other supports, including titania [14,16–18]. As a reference point for heat values, Feng and Vohs [15] reported several enthalpies of oxidation at 425 K between bulk vanadium oxides: $V_2O_3 \rightarrow V_2O_5$ $\Delta H = -343$ kJ mol $O_2{}^{-1}$, $V_2O_3 \rightarrow V_2O_4$ $\Delta H = -380$ kJ mol $O_2{}^{-1}$, $V_2O_4 \rightarrow V_2O_5$ $\Delta H = -306$ kJ mol $O_2{}^{-1}$. It is then expected that the samples with vanadia reduced to the lowest oxidation state will show the highest initial heat values. This corresponds in our study to V/R, V/RB, and V/AB samples, which indeed are samples with higher initial heats, although V/RG is also within this trend, and it does not reach a vanadia reduced state lower than V(IV). To resolve this matter further requires re-oxidation studies at higher temperatures to re-oxidize all vanadia sites, yet the association between re-oxidation heat values and degree of reduction is clearly borne out here. More importantly, the re-oxidation heat values relate directly to structural features of the surface V structures. This is especially true for the V/TiO_2–Al_2O_3 samples because of their similarity in V coverages, the extent of reduction of V species (except in the case of V/RB), and the percentage of re-oxidized sites at 473 K. The fact that the heat values are in general higher than the values for bulk re-oxidations listed above is a clear indication that the oxygen sites involved are from highly-dispersed, submonolayer V species, rather than from multilayer V. As reported in [14], vanadyl oxygens and oxygen ions that bridge vanadium ions with Al(III) support ions should be more difficult to remove or add, and thus would register higher re-oxidation heats, than oxgyens that bridge two vanadium ions. The re-oxidation heats measured in four out of the five V/TiO_2–Al_2O_3 samples averaged 480 ± 15 kJ mol $O_2{}^{-1}$. The sample V/RC gave heat values in the 400 kJ mol $O_2{}^{-1}$ range, implying that the oxygen site involved here is more labile than in the other samples.

5. Conclusions

The characterization of vanadia supported at similar loadings on several vanadium trap additives composed of pure titania and mixed titania–alumina supports showed that vanadia is stabilized as dispersed polyvanadate species and as microcrystallites of V_2O_5. As shown by TPR, the average oxidation state of vanadium is dependent upon the support material. With pure titania supports, the pure rutile preparation proved more capable than the pure anatase preparation of reducing vanadia to a low average oxidation state. Also, due to lower surface areas, vanadia coverages in these samples exceeded theoretical monolayer coverage and show more diverse vanadia reducibility. In mixed TiO_2–Al_2O_3 supports, vanadia coverages were similar and below theoretical monolayer, hence the vanadia coverage is amorphous and more uniform. Vanadia reducibility in these supports was influenced by the type of hydrated alumina precursor used, showing average oxidation states of between V(III) and V(V) following TPR, with exception to the case of the rutile-bayerite support, in which case the hydrogen consumption during TPR would correspond to reduction of vanadia to V(II). Alternatively, the support may be trapping hydrogen during the TPR experiment, although more work is necessary to substantiate this claim. Re-oxidation at 473 K of samples pre-reduced in CO at 770 K did not lead to complete re-oxidation

of reduced vanadia species, although trends in heats of re-oxidation at 473 K can be interpreted in terms of re-oxidation of the immediate surface layers, using the model mentioned in [14]. The differential heat values vary between 400 and 500 kJ mol $O_2{}^{-1}$, which are higher than the values expected for bulk re-oxidation of vanadium oxides, and give a direct measure of the oxygen–vanadium bond strengths existing on surfaces and dispersed layers of supported vanadia. These results thus showed that very similar oxygen–metal ion bond strengths (480 kJ mol $O_2{}^{-1}$) exist in the dispersed vanadia layers of the $V/TiO_2/Al_2O_3$ samples studied here, but a weaker bond-strength (400 kJ mol $O_2{}^{-1}$) operative in vanadia supported on rutile-boehmite.

Acknowledgements

The authors wish to acknowledge the assistance of Ing. Hector Solís of Industria Minera de México for assays of vanadia. Financial support from CONACyT #35106U and FIES98-23-III (Mexican Petroleum Institute) is acknowledged.

References

[1] C.A. Trujillo, U. Navarro Uribe, P.-P. Knops-Gerrits, A. Oviedo, P.A. Jacobs, J. Catal. 168 (1997) 1–15.
[2] N.P. Martínez, UK Patent 2,196,872 (11 May 1988); E.L. Kugler, US Patent 4,944,864 (31 July 1990); A. A. Chin, 5,057,205 (15 October 1991).
[3] J.B. Green, E.J. Zagula, J.W. Reynolds, L.L. Young, T.B. McWilliams, J.A. Green, Energy Fuels 11 (1997) 46–60.
[4] F. Pedraza, A. Vázquez, J. Phys. Chem. Solids 60 (1999) 445–448.
[5] J.S. Magee, M.M. Mitchell Jr., in: J.S. Magee, M.M. Mitchell (Eds.), Fluid Catalytic Cracking: Science and Technology (Stud. Surf. Sci. Catal. vol. 76), Elsevier, Amsterdam, 1993, pp. 339–384 (Chapter 4).
[6] B.E. Handy, S.B. Sharma, B.E. Spiewak, J.A. Dumesic, Meas. Sci. Technol. 4 (1993) 1350–1356.
[7] B.E. Handy, A. Baiker, M. Schraml-Marth, A. Wokaun, J. Catal. 133 (1992) 1–20.
[8] G.C. Bond, J.P. Zurita, S. Flamerz, P.J. Gellings, H. Bosch, J.G. van Ommen, B.J. Kip, Appl. Catal. 22 (1986) 361.
[9] B.H. Bosch, B.J. Kip, J.G. van Ommen, P.J. Gellings, J. Chem. Soc., Faraday Trans. I. 80 (1984) 2479–2488.
[10] G.T. Went, S.T. Oyama, A.T. Bell, J. Phys. Chem. 94 (1990) 4240–4246.
[11] B. Olthof, A. Khodakov, A.T. Bell, E. Iglesia, J. Phys. Chem. B 104 (2000) 1516–1528.
[12] Q. Sun, J. Jehng, H. Hu, R.G. Herman, I.E. Wachs, K. Klier, J. Catal. 165 (1999) 91–101.
[13] X. Gao, S.R. Bare, B.M. Weckhuysen, I.E. Wachs, J. Phys. Chem. 102 (1998) 10842.
[14] P.J. Andersen, H.H. Kung, J. Phys. Chem. 96 (1992) 3114–3123.
[15] T. Feng, J.M. Vohs, J. Catal. 208 (2002) 301–309.
[16] Z. Sobalik, R. Kozlowski, J. Haber, J. Catal. 127 (1991) 665.
[17] J.A. Odriozola, J. Soria, G.A. Somorjai, H. Heinemann, J.F. García de la Banda, M. López Granados, J.C. Conesa, J. Phys. Chem. 95 (1991) 240.
[18] N. Topsøe, J. Catal. 128 (1991) 499.